

Reentrant Phase Transformation from Crystalline Ikaite to Amorphous Calcium Carbonate

*Zhaoyong Zou, Luca Bertinetti, Wouter J.E.M. Habraken and Peter Fratzl**

Experimental Procedures

Materials and general preparative methods. Analytical grade calcium chloride dihydrate ($\text{CaCl}_2 \cdot 2\text{H}_2\text{O}$) and sodium carbonate decahydrate ($\text{Na}_2\text{CO}_3 \cdot 10\text{H}_2\text{O}$) were purchased from Sigma-Adrich. Calcium and carbonate solutions were prepared by dissolving corresponding chemicals in ultrapure water. A computer controlled titration system consisting of a titration device controlling three dosing units (800 Dosino) (905 Titrand, Metrohm Ltd.) was utilized for the experiments.

Synthesis of ACC and ikaite. The experiments were performed at $(2 \pm 1)^\circ\text{C}$ in a 100 mL vessel filled with certain amount of carbonate solution (49.5 mL) under stirring. 1 M calcium solution (0.5 mL) was dosed through the dosing unit into the reaction vessel at a rate of 10 mL per minute to ensure a rapid mixing of the two solutions, and ACC precipitated immediately. The total volume of the solution after dosing was 50 mL and the concentrations of calcium and carbonate after mixing were both 20 mM. The reaction solution was monitored by using a pH electrode and a Ca^{2+} ion-selective electrode. The precipitates were collected after crystallization

(as indicated by the pH and Ca²⁺ activity measurements) by fast vacuum filtering of the reaction solution and rinsed with ethanol. The dry powders were either characterized immediately or after storing in a vacuum desiccator.

Scanning electron microscopy. Scanning electron microscopy was performed using a field emission scanning electron microscope (JEOL, JSM-7500F) working at an acceleration energy of 10 keV. Samples were not coated prior to investigation.

Focus Ion Beam (FIB) / Scanning Electron Microscopy (SEM). FIB/SEM analysis was performed using a Zeiss Cross Beam 540 (Carl Zeiss AG, Germany). The working condition for FIB is 30 kV and 750 pA and the slice thickness is 24 nm. The image stacks are segmented using the Amira software (Visualization Sciences Group, Burlington, USA) and the porosity of the 3D volume data is calculated based on the segmentation.

Raman and infrared spectroscopy. Raman spectra were collected using a confocal Raman microscope (α 300; WITec) equipped with a CCD camera (DV401-BV; Andor), a Nikon objective (10 \times) and a 532 nm laser (40 accumulations, integration time 1s). Infrared spectra were recorded using a Thermo Scientific Nicolet is5 FTIR spectrometer (ATR-Diamond mode) (500 scans, resolution 2 cm⁻¹).

Thermogravimetric Analysis (TGA) / differential scanning calorimetry (DSC). Simultaneous weight loss and heat flow were

measured during programmed heating at 1.5 or 3 °C/min using Thermogravimetric analysis coupled with differential scanning calorimetry (SENSYS evo TGA-DSC, SETARAM Instrumentation, Caluire, France). Dry nitrogen was used as the purge gas and the flow rate varies from 20 mL/min to 200 mL/min as specified for each experiment. Approximately 10 mg

of dry powdered sample was placed in an alumina crucible with small pores on the side to promote the gas flow inside the crucible.

Small- and wide-angle X-ray scattering. Synchrotron small- and wide-angle scattering experiments were carried out at the μ -Spot beamline (BESSY II storage ring, Helmholtz-Zentrum Berlin) using a multilayer monochromator and spot size of 100 μm . 2D scattering patterns were collected using a MarMosaic CCD detector (Mar, Evanston, USA). Radial integration of the 2D scattering patterns were analyzed with the software Directly Programmable Data Analysis Kit (DPDAK), giving the spherically averaged scattering intensity as a function of the modulus of the scattering vector q , with $q = 4\pi\sin(\theta)/\lambda$ where 2θ is the scattering angle and λ is the wavelength. The resulting profiles were corrected for dark current, primary intensity and sample transmission.

Results and Discussion

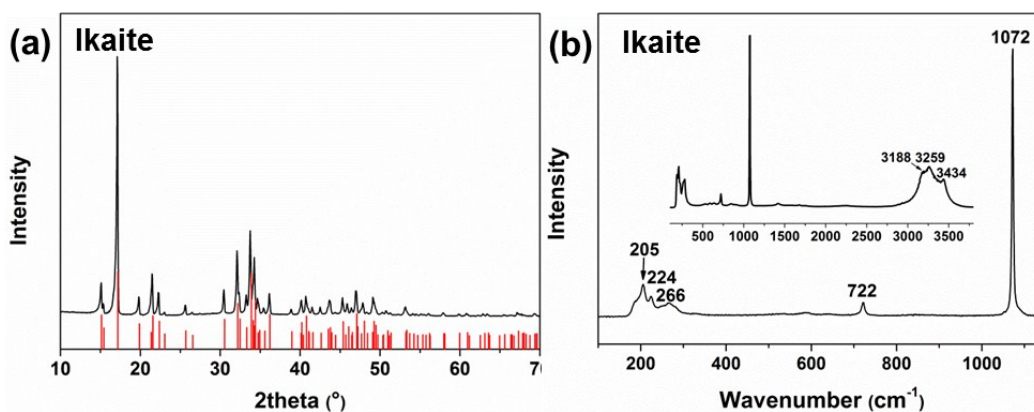


Figure S1. The XRD pattern (a) and Raman spectrum (b) of the ikaite sample after filtration.

Vertical markers below the diffraction pattern in (a) indicate the standard positions of the Bragg reflections of ikaite.

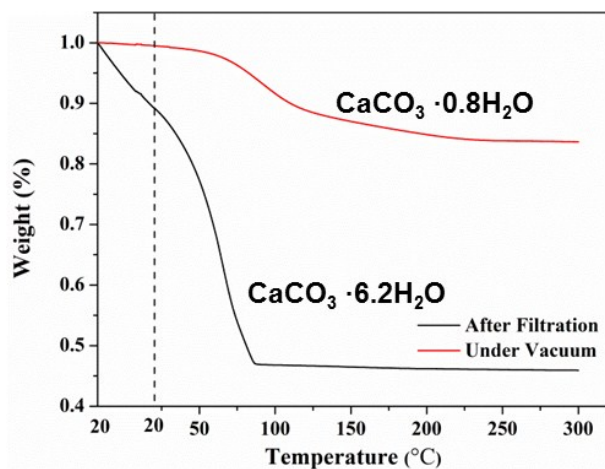


Figure S2. TGA curves of ACC after filtration and ACC after drying under vacuum.

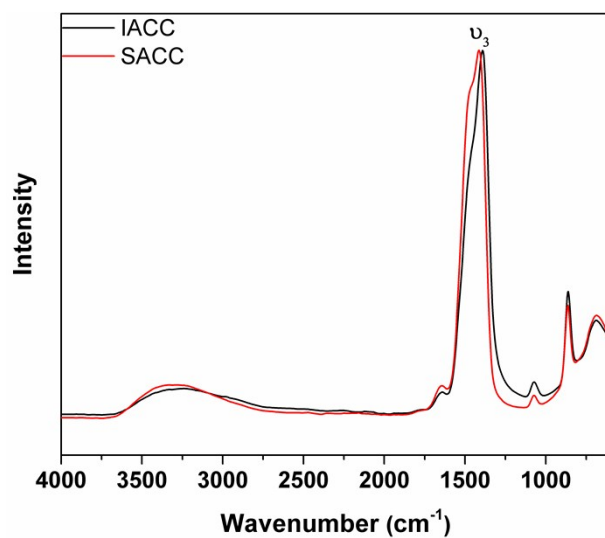


Figure S3. FTIR spectra of the ACC transformed from ikaite (IACC) and ACC synthesized from solution (SACC), showing that the peak corresponding to the asymmetric stretch ν_3 of the carbonate group for IACC at $\sim 1400\text{ cm}^{-1}$ is significantly lower than for SACC.

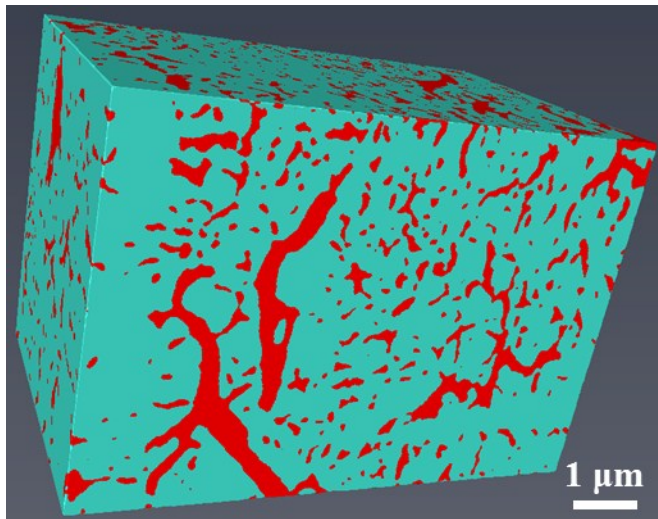
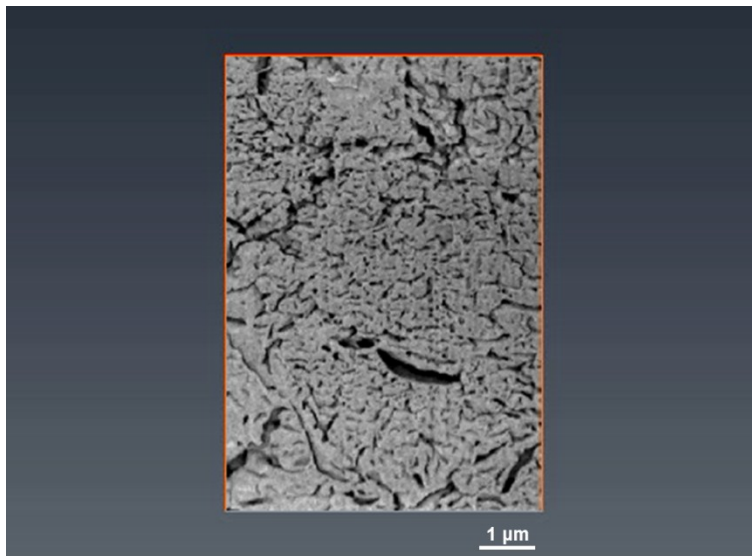


Figure S4. Surface view of after segmentation and 3D reconstruction of the FIB/SEM data, the red represents pores and channels and the green represents ACC.



Video S1. A video of the ACC, showing 259 FIB/SEM serial sections that were aligned to form a data of X=5.7 μm, Y= 8.2 μm, Z=5.4 μm, with a voxel size of 15.1 nm x 15.1 nm x 21 nm.

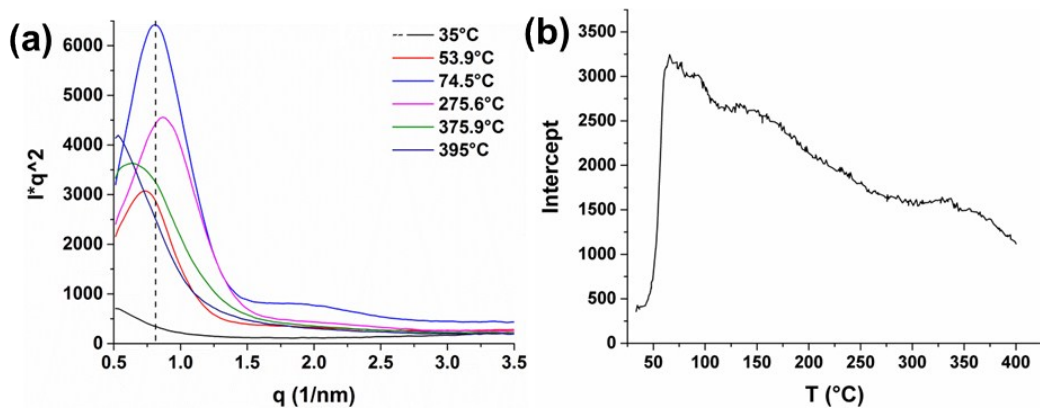


Figure S5. (a) Kratky Plot ($I \cdot q^2$ vs q) of the SAXS data at several temperatures, showing the change of peak intensity and position. (b) Plot of the intercept obtained from the linear fitting of Porod plot ($I \cdot q^4$ vs q^4) at different T , representing the change of the internal surface area of the pores.